Multiferroic properties of sol–gel derived $Bi_5Fe_{1-x}Co_xTi_3O_{15}$ thin films*

Wang Wei(王 伟), Wu Xin-Hua(武鑫华), Mao Xiang-Yu(毛翔宇), and Chen Xiao-Bing(陈小兵)†

College of Physical Science and Technology, Yangzhou University, Yangzhou 225002, *China*

(Received 30 September 2010; revised manuscript received 1 March 2011)

Co-doped $Bi_5FeTi_3O_{15}$ thin films (BFCT-x, $Bi_5Fe_{1-x}Co_xTi_3O_{15}$) were prepared using a sol–gel technique. XRD patterns confirm their single phase Aurivillius structure, and the corresponding powder Rietveld analysis indicates the change of space group around $x = 0.12$. The magnetic hysteresis loops are obtained and ferromagnetism is therefore confirmed in BFCT-x thin films. The remanent magnetization (M_r) first increases and reaches the maximum value of 0.42 emu/cm^3 at $x = 0.12$ due to the possible Fe^{3+}–O–Co^{3+} ferromagnetic coupling. When $x = 0.25$, the M_r increases again because of the dominant Fe^{3+}–O–Co^{3+} ferromagnetic coupling. The remanent polarization ($2P_r$) of BFCT-0.25 was measured to be as high as 62 μC/cm^2, a 75% increase when compared with the non-doped BFCT-0 films. The $2P_r$ remains almost unchanged after being subjected to 5.2×10^9 read/write cycles. Greatly enhanced ferroelectric properties are considered to be associated with decreased leakage current density.

Keywords: magnetism, ferroelectricity, thin film

PACS: 77.84.–s, 78.30.–j, 73.50.–h **DOI:** 10.1088/1674-1056/20/7/077701

1. Introduction

Multiferroic magnetoelctric materials, which simultaneously exhibit ferroelectricity and ferromagnetism, have recently led to a surge in the pursuit of materials having both a robust spontaneous magnetization and a large remanent polarization.[1–3] Although multiferroic composites, which incorporate both ferroelectric and ferri/ferromagnetic phases, usually yield a giant magnetoelctric coupling response, single-phase compounds are favourable to device miniaturization as well as quantum modulation between ferroelectric and ferromagnetic orders.[4] However, research of single-phase magnetoelectric materials currently remains in its infancy and faces many difficulties.[5] One of the problems is that the ferroelectric order and magnetic order are mutually expelled from the viewpoint of symmetry consideration, so the species of natural single-phase compounds are rare. Except for several compounds such as $BiFeO_3$, most of the already revealed single-phase materials exhibit a relatively low Curie temperature and Néel temperature, which hinder their industrial applications. Even $BiFeO_3$ suffers from a high leakage current and synthesis difficulties. However, the Aurivillius compound $Bi_5FeTi_3O_{15}$ (BFTO), which can be taken as an alternating stacking of $Bi_4Ti_3O_{12}$ and $BiFeO_3$ in 1:1 ratio, has again aroused attention in research circles due to the development of synthesis methods and a deeper understanding of its crystal structure and properties.[6–8] In the Aurivillius phase, Bi–O layers serve as an insulating block and as space charge storage, and the leakage current is expected to be greatly reduced compared with that of $BiFeO_3$.[9] In a BFTO structure, the magnetic order is dominated by B-site Fe ions, while the ferroelectric order is excited by A-site Bi ions and B-site Ti ions. As we reported previously, a pure BFTO thin film prepared by the same technique used here exhibited a paramagnetic nature.[10] Zhang *et al.* reported the paramagnetic nature of the BFTO ceramic target and the magnetic properties of the corresponding pulsed laser deposition (PLD)-prepared thin film remained as an open question.[11] Recently, Dong *et al.* revealed the superparamagnetic behaviour with a dominant antiferromagnetic interaction background for sol–gel derived ceramics and thin films of BFTO.[12] Until now, no evident M–H curve of a BFTO thin film has been revealed in the literature to the best of our knowledge. However, some researchers have confirmed the mag-

*Project supported by the National Natural Science Foundation of China (Grant No. 51072177) and the Natural Science Foundation of the Higher Education Institutions of Jiangsu Province, China (Grant No. 08KJB140011).

†Corresponding author. E-mail: xbchen@yzu.edu.cn

© 2011 Chinese Physical Society and IOP Publishing Ltd

netoelectric effect in BFTO compounds and pointed out that the BFTO favours the antiferromagnetic order with its Neél point T_N of about 80 K.[7−8] Based on the above, it should be a challenging task to obtain the ferromagnetic potential of BFTO at room temperature, especially in thin film form. Considering the coupling scenario in multiferroic composites, we think that ferromagnetism might be induced if an appropriate amount of magnetic ions other than Fe ions are introduced into the BFTO compound.

In this paper, we investigate the crystal structure and multiferroic properties of Co-doped $Bi_5FeTi_3O_{15}$ thin films (BFCT-x) prepared by the sol–gel route in an attempt to reveal the ferromagnetic behaviour of BFCT-x in thin film form. It is seen that ferromagnetic behaviour was successfully induced and the ferroelectric properties were also greatly improved with the addition of cobalt content up to 0.25.

2. Experiments

$Bi_5Fe_{1-x}Co_xTi_3O_{15}$ (BFCT-x, x = 0.00–0.25) thin films were fabricated on (111) Pt/Ti/SiO_2/Si/ substrates by the sol–gel deposition technique. The precursor solution was prepared by dissolving bismuth nitrate, iron (III) acetylacetonate, cobalt(II) nitrate hexahydrate and titanium n-butoxide in proportion in glacial acetic acid. Acetic acid and n-propanol were used as solvents and acetylacetone was used as a stable agent. A 3% excess of bismuth acetate was added to compensate for possible bismuth loss during the process. The films were spin-coated at 2900 rpm for 30 s and then baked twice for several minutes at temperatures of 270°C and 420°C, respectively. The as-deposited films were then submitted to an annealing treatment in a flowing nitrogen atmosphere at 680–720°C for 30 min. This process was repeated ten times to deposit the ultimate thickness of the films.

To measure the electrical properties, Pt dots with an area of 3.14×10^{-4} cm^2 were sputtered through a shadow mask toon the surfaces of the films as top electrodes. A postannealing procedure was then followed at 600°C for 10 min in an oxygen ambient to ensure Ohmic contact between Pt electrode and the films. The crystal structures of the films were analysed by X-ray diffractometer (Bruker D8) with Cu K_α radiation. The cross-sectional image and film thickness were observed using a field emission scanning electron microscope (FESEM, Hitachi, S-4800). The surface morphology and grain size of the films were observed by an atomic force microscope (AFM) (Nanoscope IIIa, Digital Instruments, USA). Raman spectra were recorded in backscattering geometry using the JY T64000 triple monochromator. A vibrating sample magnetometer (VSM) (EV-7, ADE Co., USA) was used to measure the magnetic properties. The ferroelectric properties were evaluated using Radiant Technologies RT66A and RT6000HVS standard ferroelectric test units.

3. Results and discussion

Figure 1 shows the X-ray diffraction (XRD) patterns of BFCT-x films deposited on platinum coated silicon substrates. All the patterns with different x show strong peaks corresponding to characteristic reflections of the randomly oriented four-layer polycrystalline Aurivillius phase. The insert of Fig. 1 shows the enlarged pattern with 2θ ranging from 29° to 34°. The Bragg angles relating to the main diffraction peaks such as (119) and (020) shown in the insert shift downward with increasing Co content up to 0.12. After that, they turn around and shift upwards with Co content increased to the maximum. This means that the lattice spacings calculated from these peaks first increase and then decrease with Co content and the turning point is located at x = 0.12. Furthermore, the (020) peak undergoes a process from split to overlap to split, and the turning point is also at x = 0.12. Rietveld analysis using the TOPAS program gave more information about the structural evolution of $Bi_5Fe_{1-x}Co_xTi_3O_{15}$ powders. The two space group of $Fmm2$ and $A2_1am$ were used as the starting structural model of $Bi_5FeTi_3O_{15}$.

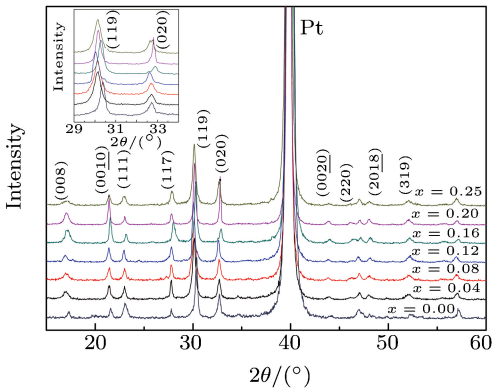


Fig. 1. XRD patterns $\theta/2\theta$ of BFCT-x thin films. Insert is the enlarged part of 2θ from 29° to 34°.

Table 1 gives the indexing results based on both $Fmm2$ and $A2_1am$. The corresponding lattice parameters are calculated based on the most fitted space group. Figure 2 shows the Rietveld analysis

of powder XRD of $Bi_5Fe_{0.88}Co_{0.12}Ti_3O_{15}$($x$= 0.12). It is seen that the $Fmm2$ space group fits better for $Bi_5FeTi_3O_{15}$ with a lower R_{wp} = 8.89. However, for x = 0.20 doping, the $A2_1am$ space group fits better than $Fmm2$ with a lower R_{wp} = 8.62. In addition, for x = 0.12, the difference of R_{wp} between $A2_1am$ and $Fmm2$ is the least, indicating that the change of space group occurs somewhere around 0.12. Furthermore, The lattice parameter a is greater than b for x = 0.00 and x = 0.08. The b is greater than a for x = 0.12 and x = 0.20, showing $a = b$ somewhere near x = 0.12, corresponding to the split and overlap of (020) peaks.

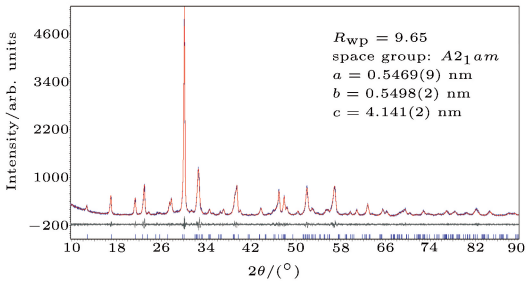


Fig. 2. (colour online) Rietveld analysis of powder XRD patterns of BFCT-0.12.

Table 1. R factors and structural data of $Bi_5Fe_{1-x}Co_xTi_3O_{15}$ powders.

x	R_{wp} /%		R_p /%		Lattice parameters		
	$Fmm2$	$A2_1am$	$Fmm2$	$A2_1am$	a /nm	b /nm	c /nm
0.00	8.89	12.13	6.71	9.85	0.5500(3)	0.5457(1)	4.145(7)
0.08	9.12	11.21	6.86	9.12	0.5585(2)	0.5555(4)	4.157(7)
0.12	10.41	9.65	8.12	7.02	0.5469(9)	0.5498(2)	4.141(2)
0.20	13.21	8.62	10.12	6.47	0.5463(2)	0.5497(2)	4.174(2)

Notes: R_p is the profile and R_{wp} is the weighted profile.

Figure 3 presents the FESEM cross-sectional image of BFCT-0.12 in a scale of 2 μm. It reveals a clear and sharp boundary between the film and Pt electrodes, suggesting no evident inter-diffusion across the capacitor structure. It is seen that the film has a uniform thickness of about 450 nm. The surface morphology of the BFCT-0.25 thin films probed by AFM is shown in the insert of Fig. 3. Throughout the observed area of 16 μm × 16 μm, the film is uniform, smooth, crack-free and has a dense island-like microstructure. The surface rms roughness of the BFCT-0.25 thin films is 13.82 nm by measuring the height of grains aligning along the 22.4-μm-long diagonal of the investigated square. The cobalt modification does

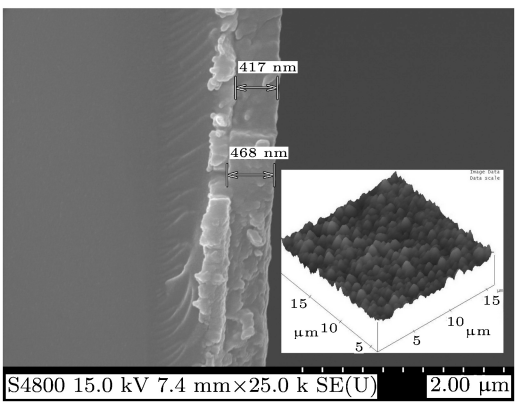


Fig. 3. SEM cross-sectional image of BFCT-0.12. Insert is the AFM picture of BFCT-0.25.

not significantly change the grains and morphology due to the similar ionic radius of Fe^{3+} (0.64 Å) and Co^{3+} (0.63 Å).

Figure 4 shows the room-temperature-recorded Raman spectra of the BFCT-x thin films. The overall shape of BFCT-x is analogous to that of $SrBi_4Ti_4O_{15}$.[13] Based on the simple mass consideration in $SrBi_4Ti_4O_{15}$, the strongest and sharpest mode observed at about 60 cm^{-1} is recognized as a rigid mode depicting the displacement of Bi^{3+} ions in Bi_2O_2 layers, and the triplet bands at 102.2, 120.5 and 152.2 cm^{-1} are the modes originating from the motion of A-site ions in the pseudo-perovskite slabs. The mode at around 270 cm^{-1} corresponds to the torsional bending of TiO_6 octahedra and the modes above 800 cm^{-1} are related to the stretching modes of TiO_6 octahedra.[14−16] In the BFCT-x films, the mode corresponding to Bi_2O_2 layers is at 61 cm^{-1}, indicating that the FeO_3 octahedra does not affect the Bi_2O_2 layers. As for the A-site motion related modes in the BFCT-x thin films, only the 117 cm^{-1} mode is prominent. It is reasonable that only Bi ions occupy the A-sites of BFCT-x while Sr and Bi ions randomly occupy the A-sites of $SrBi_4Ti_4O_{15}$. The high-frequency internal modes above 200 cm^{-1} of BFCT-x films can also find their counterparts in $SrBi_4Ti_4O_{15}$ with slight Raman shifts. The coincidence of the Raman modes indicates that the BFCT-x and $SrBi_4Ti_4O_{15}$ have a similar Aurivillius structure. However, in $SrBi_4Ti_4O_{15}$, we cannot observe the 683 cm^{-1} mode which is obvious in BFTO films. The origin of this mode may

be due to the following: (i) this mode was not observed in Aurivillius phases without FeO_6 octahedra and thus it should be related to FeO_6 octahedra; (ii) this mode was observed clearly in orthorhombic $LaFeO_3$ and rhombohedral $LaMnO_3/LaCoO_3$ but was not observed in rhombohedral $BiFeO_3$.[17,18] As is well known, substitution of La for Bi ions may reduce the lattice distortion in perovskites due to the 6s lone pair electrons of Bi ions.[19] Therefore, the appearance of this mode might be related to octahedra containing magnetic ions (Fe/Mn/Co) and/or lower lattice symmetry such as orthorhombic and/or relaxed rhombohedral. As we can see in Fig. 3, the mode at 683 cm^{-1} exhibits a broadening tendency with increasing cobalt content while the frequency shift is almost negligible. Due to the similar ionic radii of Fe^{3+} and Co^{3+}, the substitution of an amount of cobalt up to 0.25 does not lead to a detectable frequency shift. However, the cobalt substitution for Fe^{3+} brings about the local ionic disorder and therefore causes the magnetic ion-related Raman mode to become broader.[20] It is also observed that the A-site ion related Raman mode splits a little when the cobalt content is higher than 0.12, indicating that the A-site ions are affected thereafter.

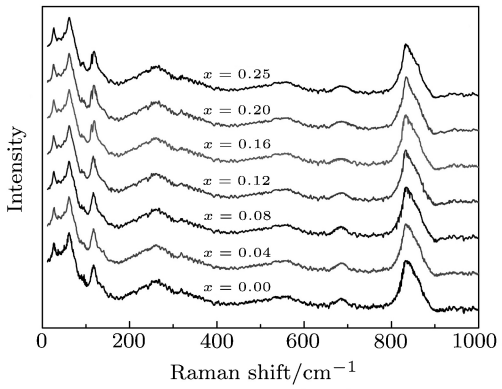


Fig. 4. Raman spectra of BFCT-x recorded at room temperature.

Figure 5 shows the M–H curves of BFCT-x thin films under an applied magnetic filed of 6 kOe (1 Oe = 79.5775 A/m) at room temperature and the dependences of remanent magnetization (M_r) and the coercive field (H_c) on the cobalt content. The BFCT-x films are saturated and exhibit square hysteresis loops, indicative of a distinct switching field. It is seen that the M_r increases with a rise in Co content up to 0.12 and then decreases with further increasing Co content. However, when Co content is increased to 0.25, the M_r turns to increase again. The saturated magnetization (M_s) shows a similar variation to that of M_r. The H_c undergoes a monotonic decrease except for a sudden rise at $x = 0.12$. Our experimental results of cobalt modification in BFCT-x thin films have brought the M_r from zero at $x = 0$ to fairly high 0.42 emu/cm^3 at $x = 0.12$ (1 emu = 10^{-3} A·m^2), indicating that ferromagnetism at room temperature has been successfully induced. In line with the empirical rule that the magnetic performance is dominated by TM ions at the B-site with partially filled shells in the perovskite structure, the promotion of the weak ferromagnetism should be closely related to the role of Fe and Co ions, such as their chemical valence state and the spatial distribution and alignment. In pure BFTO, the main cause for the failure in probing the M–H curve is associated with the antiferromagnetic superexchange interactions of Fe^{3+}–O–Fe^{3+} due to the paramagnetic nature of Fe^{3+} ion.[21] By substituting a certain amount of Co ions for Fe^{3+} ions, the Fe^{3+}–O–Fe^{3+} interaction is suppressed and the balance between the anti-parallel magnetization at Fe^{3+} sublattices is upset to some extent. From micro-structural points of view, the Fe^{3+} ions have a probability to couple the Co^{3+} ions via the oxygen ions at the apexes of the octahedron from directions parallel to the c axis, as well as in the ab plane of the unit cell. Such Fe^{3+}–O–Co^{3+} interaction might be ferromagnetic and results in a locally ordered magnetic structure, which contributes a large part to the macro-magnetization, i.e. ferromagnetism.[22]

Apart from the ferromagnetic coupling, other factors may also exert influence on the enhanced magnetization. The valence fluctuation of Fe/Co ions has been widely demonstrated in perovskite structures. The existence of Fe^{2+} ions would possibly cause a double exchange interaction in the Fe^{2+}–O–Fe^{3+} chain, which may result in an enhancement of ferromagnetism. In addition, the introduction of a certain amount of cobalt into the B-site could inevitably lead to distortion of the crystal structure and change the angle of the Fe–O–Fe bond, resulting in the occurrence of net magnetization in the material. In our experimental results, an interesting phenomenon was found: when $x = 0.25$, the M_r as well as the M_s resume their increasing tendency after the decrease starting from $x = 0.12$. When x is increased from zero to 0.12, cobalt ions occupy the B-site and the ferromagnetically coupling between Fe^{3+} and Co^{3+} plays a crucial role in the enhancement of magnetization. When the cobalt content is increased to a value higher than 0.12, some divalent cobalt ions might affect the A-sties and cause structural relaxation and the decrease of M_r. When the cobalt content is increased to 0.25, the Fe^{3+}–O–Co^{3+} coupling becomes more prominent and offsets the decrease of M_r caused by structural relaxation.

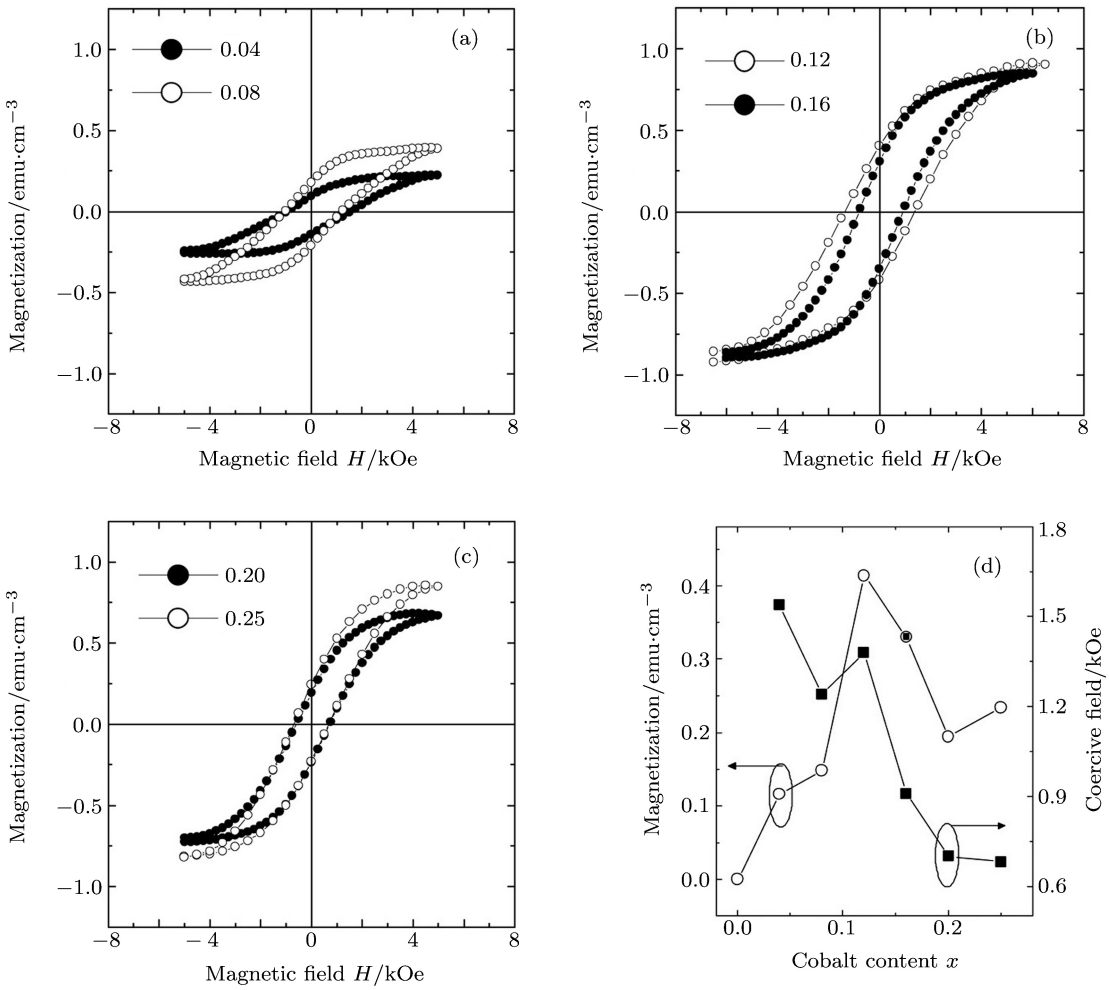


Fig. 5. (a)–(c) The M–H hysteresis curves of BFCT-x thin films and (d) the variation of M_r and H_c on cobalt content (d).

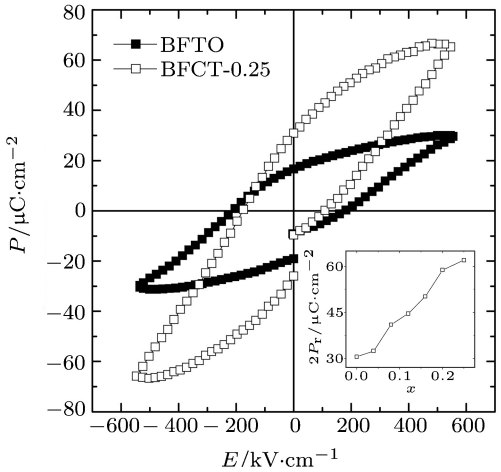


Fig. 6. The P–E hysteresis loops of BFCT-0 and BFCT-0.25 thin films.

Figure 6 compares the P–E hysteresis loops between the BFCT-0 and BFCT-0.25 thin films, and the insert plots the dependence of $2P_r$ on cobalt content. The as-grown films can bear a high electric field without breakdown, indicating the high quality of the films.[23] In addition, a good intimate Ohmic contact between the electrodes and the substrate, as can be observed in the SEM cross-sectional picture, may contribute to the voltage endurance. From the insert, it can be seen that the $2P_r$ is monotonically increased with a rise in the doping Co content. The $2P_r$ of BFCT-0.25 was measured to be as high as 62 μC/cm^2, a 75% increase when compared with the nondoped BFCT-0 films. Meanwhile, the coercive field (E_c) was decreased from 171 kV/cm to 142 kV/cm, indicative of well-improved ferroelectric property resulting from cobalt doping.

Figure 7 presents the results of the fatigue tests of BFCT-0 and BFCT-0.25 performed at room temperature using a 50 kHz bipolar square wave and the corresponding hysteresis loops before (opened circle) and after (filled circle) being subjected to 5.2×10^9 read/write cycles. The polarization of the BFCT-0 film decreased to 66% while that of the BFCT-0.25 remains almost unchanged. The cobalt doping has greatly improved the material's fatigue endurance properties.

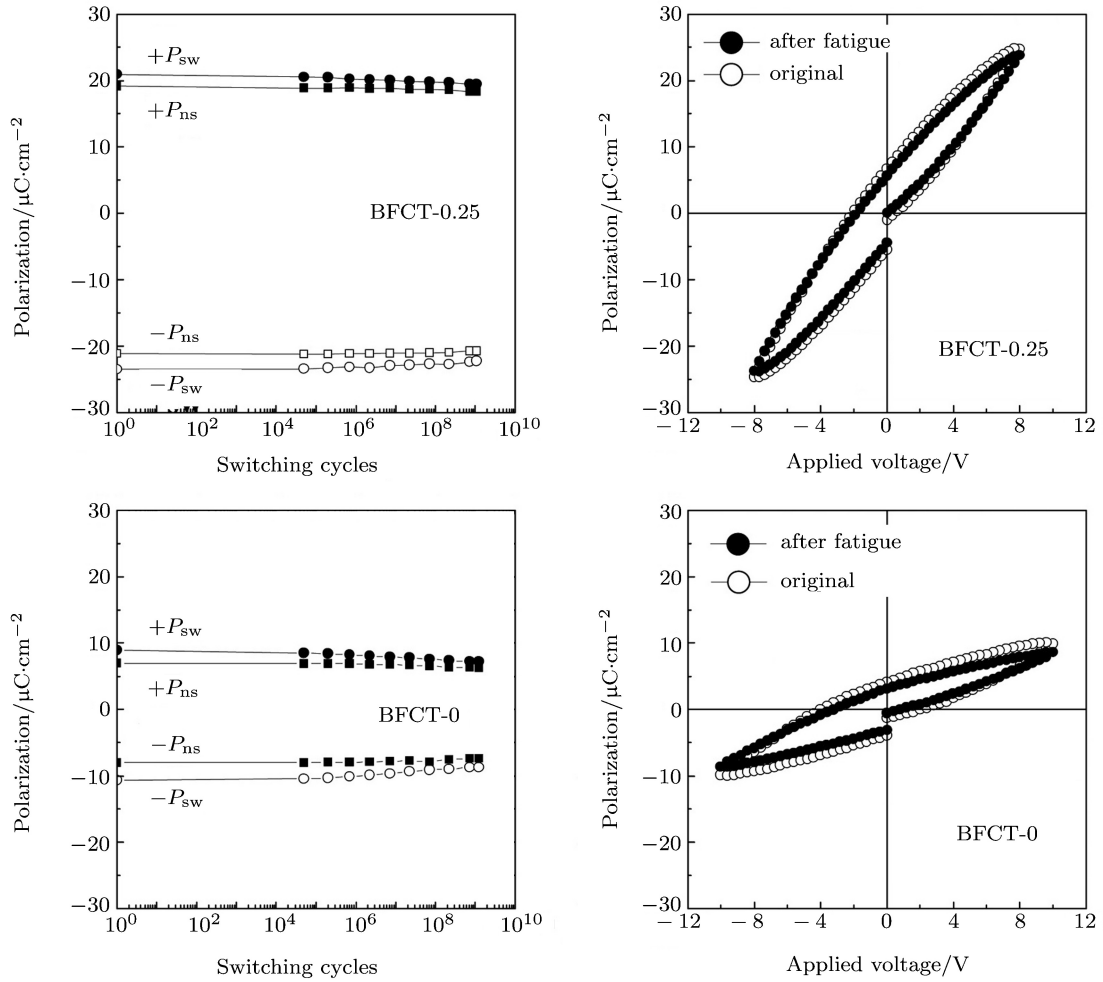


Fig. 7. Fatigue behaviour of (a) BFCT-0 and (c) BFCT-0.25 thin films and their hysteresis loops (b) before and (d) after fatigue test. P_{sw} is the switchable polarization and P_{ns} is the non-switchable polarization.

Figure 8 shows the typical electric-field dependence of the leakage current density (J–E) of the BFCT-0 and BFCT-0.25 thin films. The dc voltage was applied in a 0.1 V step. A 10-s soak time between two adjacent steps was used to ensure steady-state measurement. The overall shapes of the two films are quite similar, except that the 0.25 content cobalt addition leads to an evident decrease of leakage current in the BFCT-0.25 compared with the BFCT-0 film. The current densities of both films increase linearly with the applied electrical field in the low strength region (below∼28 kV/cm), suggesting ohmic conduction. At a higher field, from about 50 kV/cm to about 200 kV/cm, the conduction mechanisms in both cases seem to be governed by Schottky emission, as described by the linear relationships of ln$J$ and $E^{1/2}$ to the experimental data, as shown in the upper insert of this figure.[24] The curves of ln$J$ versus $E^{1/2}$ deviate from the linear trend for the applied field higher than ∼200 kV/cm, implying that different conduction mechanisms dominate this high electric field regime. It is hard to distinguish the conduction mechanism in this high field regime, because none of the three most important conduction relations, including space-charge-limited current (SCLC), Schottky and Poole–Frenkel, fit well with the measured data

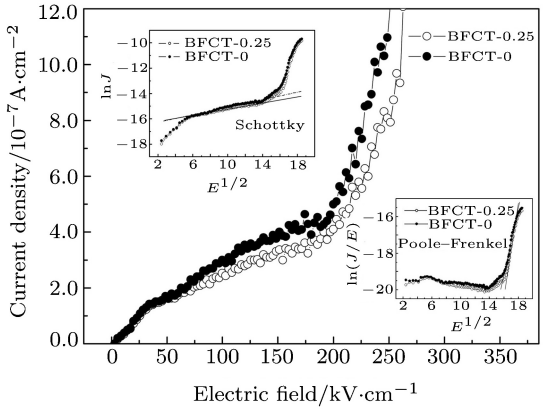


Fig. 8. The electric field dependence of leakage current density of BFCT-0 and BFCT-0.25 thin films. The inserts show the plots of ln$J$ versus $E^{1/2}$ for Schottky emission and ln$J$ versus $E^{1/2}$ for Poole–Frenkel emission. E is in the unit of kV/cm and J is in the unit of A/cm^2.

in the whole field ranging from about 200 kV/cm to breakdown, although a Poole–Frenkel relation coincides well with the data in a narrow field interval from about 268 kV/cm to about 306 kV/cm, as shown in the lower insert of this figure. It is well known that the Poole–Frenkel emission mechanism is bulk limited and excludes the interface-limited Schottky emission mechanism. Since Schottky emission governs the main field range, the Poole–Frenkel fitting is therefore doubtful. It might be the co-effect of several conduction mechanisms. Further investigations and analysis of the conduction mechanisms in this field are needed. For one thing, the isovalent substitution of Co^{3+} for the Fe^{3+} ions in BFCT-x thin films may facilitate the crystallization and mobility of the domain walls. In addition, Fe ions and Co ions are both known to be multivalent and nominal isovalent substitution could not totally exclude the probability of the aliovalent substitution of Co ions for Fe ions, especially at higher doping contents, although at the present stage we cannot point out the exact substitution scenario between Co^{2+}, Co^{3+} and Fe^{2+}, Fe^{3+} and Fe^{4+} ions. The leakage current density results indicate that the possible aliovalent substitution may lead to the decrease of the point defects. The reduced leakage current is therefore responsible for the greatly enhanced polarization and well improved fatigure endurance.

4. Conclusion

The structural, magnetic and ferroelectric properties of cobalt modified $Bi_5FeTi_3O_{15}$ thin films (BFCT-x) have been investigated in this paper. It is found that the remanent magnetization (M_r) was increased to 0.42 emu/cm^3 at $x = 0.12$ and ferromagnetism was induced due to the possible Fe^{3+}–O–Co^{3+} ferromagnetic coupling. When $x = 0.25$, the M_r increases again because of the dominant Fe^{3+}–O–Co^{3+} ferromagnetic coupling. The remanent polarization ($2P_r$) of BFCT-0.25 was measured to be as high as 62 μC/cm^2, a 75% increase when compared with nondoped BFCT-0 films. The $2P_r$ remained almost unchanged after being subjected to 5.2×10^9 read/write cycles. Greatly enhanced ferroelectric properties were considered to be associated with decreased leakage current density.

References

[1] Fiebig M 2005 *J. Phys.* D: *Appl. Phys.* **38** R123

[2] Hill N A 2000 *J. Phys. Chem.* B **104** 6694

[3] Wang J, Neaton J B, Zheng H, Nagarajan V, Ogale S B and Liu B 2003 *Science* **299** 1719

[4] Nan C W, Bichurin M I, Dong S, Viehland D and Srinivasan G 2008 *J. Appl. Phys.* **103** 031101

[5] Wang K F, Liu J M and Ren Z F 2009 *Adv. Phys.* **58** 321

[6] Kubel F and Schmid H 1992 *Ferroelectrics* **129** 101

[7] Srinivas A, Suryanarayana S V, Kumar G S and Kumar M M 1999 *J. Phys.*: *Condens Matter* **11** 3335

[8] Singh R, Bhimasankaram T, Kumar G S and Suryanarayana S V 1994 *Solid State Commun.* **91** 567

[9] Kim S K, Miyayama M and Yanagida H 1996 *Matter. Res. Bull.* **31** 121

[10] Wang W, Sun J B, Mao X Y and Chen X B 2008 *J. Phys.* D: *Appl. Phys.* **41** 155418

[11] Zhang S T, Chen Y F, Liu Z G, Ming N B, Wang J and Cheng G X 2005 *J. Appl. Phys.* **97** 104106

[12] Dong X W, Wang K F, Wan J G, Zhu J S and Liu J M 2008 *J. Appl. Phys.* **103** 094101

[13] Jin C, Zhu J, Mao X, He J and Chen X 2006 *Acta Phys. Sin.* **55** 3716 (in Chinese)

[14] Sugita N, Osada M and Tokumitsu E 2002 *Jpn. J. Appl. Phys.* **41** 6810

[15] Hu X, Wang W, Mao X and Chen X 2010 *Acta Phys. Sin.* **59** 8160 (in Chinese)

[16] Osada M, Tada M, Kakihana M, Watanabe T and Funakubo H 2001 *Jpn. J. Appl. Phys.* **40** 5572

[17] Singh M K, Jang H M, Ryu S and Jo M H 2006 *Appl. Phys. Lett.* **88** 042907

[18] Popa M, Frantti J and Kakihana M 2002 *Solid State Ionics* **154-155** 135

[19] Shimakawa Y, Kubo Y, Tauchi Y, Asano H, Kamiyama T and Izumi F 2001 *Appl. Phys. Lett.* **79** 2791

[20] Zhu J, Mao X and Chen X 2004 *Acta Phys. Sin.* **53** 3929 (in Chinese)

[21] Naganuma H, Miura J and Okamura S 2008 *Appl. Phys. Lett.* **93** 052901

[22] Mao X, Wang W, Chen X and Lu Y 2009 *Appl. Phys. Lett.* **95** 082901

[23] Wu Y Y, Wang X H and Li L T 2010 *Chin. Phys.* B **19** 037701

[24] Pabst G W, Martin L W, Chu Y H and Ramesh R 2007 *Appl. Phys. Lett.* **90** 072902